

Influencing Parameters on Discharge Bearing Currents in Inverter-Fed Induction Motors

Thibaud Plazenet , Thierry Boileau , Cyrille Caironi, *Member, IEEE*,
and Babak Nahid-Mobarakeh , *Senior Member, IEEE*

Abstract—This article investigates discharge bearing currents in inverter-fed electric motors. Industrial reports indicate that among prevalent bearing failures, bearing currents are one of the influent drivers leading to a variety of tribological issues and premature wear in bearings. While the root-causes of bearing currents have been extensively reported over the years, the response of bearing under voltage stress and the factors that influence bearing endangerment through electric discharges have been far less studied. An online measurement of the bearing voltage is proposed on a motor test-bench to estimate both the discharge activity and the energy of the discharges. The designed test bed allows reproduction of representative bearing currents leading to electrical micropitting. This paper presents extensive measurements results that highlight the critical operating conditions and parameters that worsen the discharge phenomenon inside bearings. Testing protocols are performed to quantify the influence of each parameter separately. While the bearing voltage magnitude play a significant role in the discharge phenomenon, other parameters such as successive startups, bearing temperature, and type of grease deserve appropriate investigations to avoid or mitigate the well-known shortened bearing life under inverter operation.

Index Terms—Bearings (mechanical), inverter-induced bearing currents, EDM bearing currents, common mode voltage, discharge, breakdown voltage, variable-frequency drives.

I. INTRODUCTION

NOWADAYS, variable speed drives are widely used in industry to control low voltage induction motors in the range of a few kW. It has been well recognized that these motors are more prone to suffer from additional bearing damage that could significantly reduce their reliability. Several studies have reported that one of the main bearing damage in this configuration is associated to Electric Discharge Machining (EDM) bearing currents (e.g. [1]–[10]). Over the years, authors have analyzed the cause-and-effect chains for this bearing damage (e.g.

Manuscript received April 7, 2020; revised July 15, 2020; accepted August 17, 2020. Date of publication August 24, 2020; date of current version May 21, 2021. This work was supported by the Université de Lorraine, CNRS, LEMTA, F-54000, Nancy France. Paper no. TEC-00203-2020. (*Corresponding author: Thibaud Plazenet.*)

Thibaud Plazenet and Thierry Boileau are with the Université de Lorraine, CNRS, LEMTA, F-54000 Nancy, France (e-mail: thibaud.plazenet@univ-lorraine.fr; thierry.boileau@univ-lorraine.fr).

Cyrille Caironi Boileau is with the CAIRCY, F-54160 Pulligny, France, and also with the Power Diagnostic Service Switzerland, GmbH, 8954 Geroldswil, Switzerland (e-mail: cyrille.caironi@caircy.org).

Babak Nahid-Mobarakeh is with the McMaster University, Hamilton, Canada, and also with the Université de Lorraine, GREEN, F-54000 Nancy, France (e-mail: babak.nahid@univ-lorraine.fr).

Color versions of one or more of the figures in this article are available online at <https://ieeexplore.ieee.org>.

Digital Object Identifier 10.1109/TEC.2020.3018630

[11]–[15]) in order to apply mitigation techniques against EDM bearing currents. Researches have been conducted to better understand the damage mechanism that takes place inside the bearing due to electric currents [15]–[20]. Electrical micropitting of the bearing steel along with lubricant ageing are usually reported and result in broader types of bearing damage such as pitting or the well-known fluting patterns (e.g. [18], [19], [21]–[25]).

However, today the phenomena that lead to bearing damage are not fully understood in a satisfactory manner [26]. Previous research [26]–[31] studied the influence of bearing temperature, bearing load, bearing grease, motor speed, inverter switching frequency and dc-link voltage on the frequency of occurrence of discharge bearing currents, EDM bearing current magnitude, and bearing impedance. Few studies (e.g. [6], [28]) have been performed to analyze any possible correlation between operating parameters and the energy released by EDM events for a given time of operation. In this study, we aim to contribute to a better understanding of the bearing electric behavior and a better quantification of the influencing parameters on the energy released by EDM bearing currents. The knowledge of conditions that mostly favorize the presence of EDM bearing current could be a great advantage to avoid the most critical operating conditions and to contribute to the design of innovative mitigations techniques at minimum cost. This paper investigates the electrical behavior of bearings submitted to electrical stress during laboratory test runs. The electrical stress is designed to be representative of a typical industrial application (i.e. a low power motor fed by an inverter). We focused on any kind of parameters that could stimulate EDM events inside a bearing such as successive startups, bearing voltage magnitude and frequency along with bearing temperature and grease type. Such test-runs had produced EDM bearing currents that led to electrical micropitting. We first review the discharge bearing current phenomenon, and present the proposed online measurement technique along with the test setup.

II. CONTEXT

A. Review of Inverter-Induced Discharge Bearing Currents

The generation of EDM bearing currents with fast switching inverter operation is due to a capacitive coupling effect inside the motor. The rise time of power semiconductors are short and leads to high dv/dt . Under this configuration, the common mode voltage produced at the stator terminals contain high-frequency components that interact with the parasitic capacitances of the

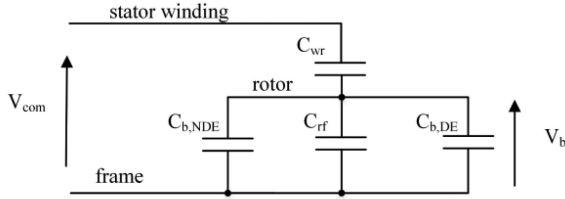


Fig. 1. Equivalent circuit for the determination of the bearing voltage of an AC motor.

machine [32]. When the bearing lubricant form an insulating layer between the rolling elements and the raceways above a certain motor speed (around 10% of rated speed), the bearing voltage mirrors the common mode voltage through a capacitive voltage divider (Fig. 1). The parasitic capacitances between the rotor and the frame, C_{rf} , the winding and the rotor, C_{wr} , and the bearing capacitances, $C_{b,DE}$ and $C_{b,NDE}$ (of the drive end and non-drive end) are responsible of the bearing voltage build-up. The capacitance of the lubricant is charged until the electric field strength surpasses the lubricant breakdown strength which causes an electrical breakdown or “discharge” which lead to the formation of an EDM-current pulse i_b . The energy stored in the parasitic capacitances discharges through the bearing resistance R_b . This discharge current i_b with peak amplitudes from 0.5 to 3 A produces a degradation of raceways, rolling elements, and lubricant [19], [33]. The presence of a voltage superior to the threshold voltage (i.e. the breakdown voltage) of the bearing is not a sufficient condition for the appearance of an EDM-event. A breakdown is dependent on the physico-chemical properties of the dielectric between the rolling elements and the races e.g. metallic particles in the lubricating film) and the quality of the contact area (micro-asperities). Furthermore, it has been reported in [26], [34] that the lubricant is conductive after each breakdown and needs a sufficient amount of time to recover its insulating properties before the appearance of the next breakdown. Therefore, a breakdown is a stochastic event by nature and can occur thousands of time per second in both bearings of the motor. It is reported by several authors that the discharges result in small craters (0.5 to 8 μm) on the raceways depending on energy dissipated [15], [35], [36].

B. Evaluation of the Discharge Phenomenon

The Bearing Voltage Ratio (*BVR*) of a motor is an important electrical parameter that estimates the probability of occurrence of discharges and bearing voltage amplitude [37]. It is mainly determined by the parasitic capacitances of the motor. The bearing voltage magnitude V_b can be estimated with the measurement of the common mode voltage and determination of the *BVR* [37].

$$V_b = BVR \cdot V_{com} = \frac{C_{wr}}{C_{wr} + C_{rf} + 2C_b} \cdot V_{com}. \quad (1)$$

However, the *BVR* is not precise enough to characterize the discharge phenomenon that takes place inside the bearing since it does not take into account lubricating conditions. To quantify the frequency of occurrence of the bearing currents, the discharge activity (*DA*) have been introduced [35]. As the occurrence of a discharge is a stochastic event that depends on the lubricant’s

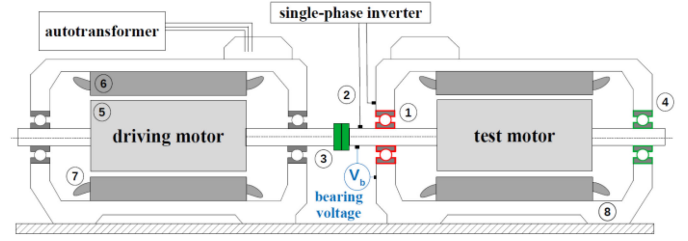


Fig. 2. Layout of the laboratory test bench. 1) Test bearing (in red); 2) Inverter’s connections; 3) Insulated coupling (in green); 4) Ceramic bearing (in green); 5) Rotor; 6) Stator; 7) Winding; 8) Frame.

behavior, the *DA* (expressed in s^{-1}) is computed on a large time window (usually around 30 s) to average its short-term variations [29]. It has been extensively utilized through radio-frequency (RF) measurements, by detecting the energy radiated outside the motor bearings during a discharge (e.g. [20], [29], [34], [38]). However, the use of this indicator alone does not provide information on the discharged energy in the bearing.

Different methods can be employed to calculate the energy released in the bearing during a discharge. It have been proposed in [21] to measure both discharge current and voltage and compute W_{dis} on the duration of current flow:

$$W_{dis} = \int V_b(t) i_b(t) dt. \quad (2)$$

This method implies an intrusive measurement of bearing voltage and bearing current and a specially designed end-shield motor to set up the current probe near the bearing [28], [35]. As stated in [6], [38], [39], it is possible to compute the discharge energy W_{dis} with the equivalent parasitic capacitance C_{tot} and the bearing voltage at breakdown V_{bd} :

$$W_{dis} = \frac{1}{2} C_{tot} V_{bd}^2. \quad (3)$$

From the capacitive equivalent circuit of the machine (Fig. 1), we can express $C_{tot} = C_{rf} + C_{b,DE} + C_{b,NDE}$. The energy of a discharge is not known using (1) since it only estimates a theoretical maximum breakdown voltage. Moreover, depending on bearing lubricating conditions, such maximum could never be reach.

III. EQUIPMENT AND MEASUREMENT METHODS

A. Laboratory Setup

The test bench comprises a low voltage squirrel cage induction motor (3-phase, 7.5 kW, 4-pole) and a similar driving machine coupled with an insulated coupling. The drive end (DE) bearing of the test motor is a brand new 6208 2Z C3 deep groove ball bearing greased for life. The non-drive end (NDE) bearing has ceramic balls, thus capacitive discharges are only allowed in the test bearing. The test bench is operated via the driving machine at a constant load due to rotor weight (Fig. 2). Before operating the test rig, a running-in phase is performed by operating the driving machine for 6 hours at its nominal speed (1500 rpm) in order to homogenize the grease repartition of the test bearing. For bearing temperature estimation, a PT1000 temperature sensor is fixed on the motor frame in the vicinity of the outer bearing

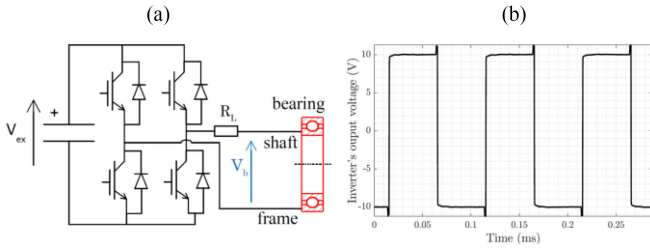


Fig. 3. (a) Diagram of the inverter allowing capacitive discharge in the rotating bearing; (b) Inverter's output voltage waveform, $V_{ex} = 10$ V and $f_{ex} = 10$ kHz without bearing.

race. This temperature indicator provides only an image of the bearing outer race temperature; however, its usage is legitimate for relative comparison of temperatures.

B. Generation & Measurement of Capacitive Discharges

We place the test bearing within conditions that allow the appearance of capacitive discharges. In order to tune precisely the amplitude and frequency of the bearing voltage when the bearing is rotating, we employ a single-phase inverter directly connected to the test bearing. The inverter is wired between the motor shaft (by means of a conductive microfiber brush) and the frame near the test bearing. This setup will be representative of the bearing behavior of a low power motor fed by an inverter if the following conditions are met:

- 1) The voltage applied at the bearing is similar to the bearing voltage build-up related to the common mode voltage (see Section II.A).
- 2) The energy of the discharges is limited to typical values of such application.
- 3) High-frequency circulating currents are negligible.

The output voltage of the inverter is a square wave voltage mimicking the bearing voltage resulting from the capacitive voltage divider (Fig. 1). The rise time of the inverter's output voltage (Fig. 3(b)) is similar to the one of typical drive systems. ($T_{rise} = 85$ ns). The bearing resistance R_b is estimated between 4 and 47 Ω for bearing thermal steady-state around 22 $^{\circ}$ C. Thus, a high resistance $R_L \gg R_b$ is set up at the output of the single-phase inverter (Fig. 3) to limit the output current at a negligible level when the bearing lubricant presents a resistive mode [26]. The bearing voltage can still build up through the $R_L C_{tot}$ circuit in order to generate discharges in the bearing. The discharge energy is representative of an industrial application since the inverter is charging the parasitic capacitances C_{tot} of a typical low power motor. When a discharge occurs, the discharge current is only provided by the parasitic capacitances of the motor since the current from the inverter is limited by the resistance R_L .

Consequently, this setup reproduces the typical electric bearing behavior of a low-power drive system. The magnitude of the applied voltage V_{ex} should be sufficiently high to surpass the breakdown voltage V_{bd} of the lubricant. In literature, the typical dielectric strength E_{bd} of bearing lubricant is around 15 V/ μ m [23] and given a lubricant thickness range of 0.2 to 2 μ m, the lubricant film discharges at $V_b \approx [3, 30]$ V.

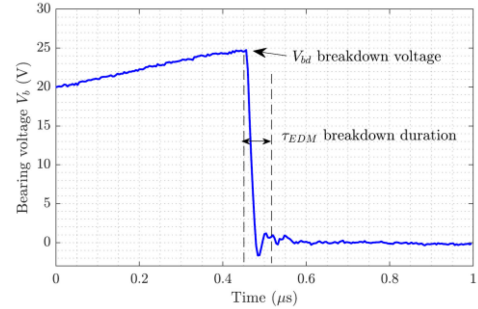


Fig. 4. Example of a measured capacitive discharge in the test bearing when the motor is run with an inverter; Sampling frequency $F_{ech} = 250$ MS/s.

The bearing voltage is measured with an oscilloscope voltage probe (Fluke VPS200) modified with a conductive microfiber tip to ensure continuous contact with the rotating shaft. The probe is installed between motor shaft and frame as close as possible from the test bearing. The measurement equipment consisted in a DPO5054 oscilloscope connected to the local network to perform online discharge analysis during motor operation: discharge activity and discharge energy estimations. Both parameters have to be considered for an accurate assessment of EDM bearing currents. Compared to non-intrusive RF technique which counts the RF pulses originated from the discharges [29], [38], without measuring the discharge energy, the proposed intrusive method allows both the estimation of the discharge activity and the dissipated energy in the bearing during motor operation. The novelties of the proposed measurement method are detailed in the following sections.

C. Discharge Activity Estimation

We estimate the discharge activity by detecting and counting discharges in a defined time window. The sampling frequency of the oscilloscope must be high enough to detect accurately a discharge and low enough to record events in a large time window. Thus, the sampling frequency was set to $F_{ech} = 12.5$ MS/s which seems the best trade-off with the equipment used. The test motor, prior to subsequent tests, is run with its inverter to observe the discharge phenomenon. The largest breakdown voltage measured on the test bearing is 25 V peak (Fig. 4). Discharge's shapes are mostly identical and can be characterized by a fast voltage drop from the breakdown voltage to approximately zero volt. This is consistent with previous measurements provided by literature [28], [34]. The duration τ_{EDM} of EDM events is ranging from 80 to 240 ns on the test bearing. In order to detect a discharge, we run a simple algorithm [40] that identify each voltage drop in the range of τ_{EDM} and superior to a defined detection threshold $V_{th} = 1.5$ V which is set slightly higher than the noise voltage (Fig. 5). A test is performed to validate our detection algorithm. The excitation voltage is set to $V_{ex} = 10$ V to favor breakdown of lubricant film. The detection algorithm counts accurately discharges such as $V_{bd} > V_{th}$ (Fig. 5). Results presented in this paper can be compared since the same threshold V_{th} value is applied for all measured signals. Due to the stochastic nature of the lubricant film breakdown, the discharge activity DA_m is measured on a long observation window ($t_m = 28$ s) to average out its variations [29].

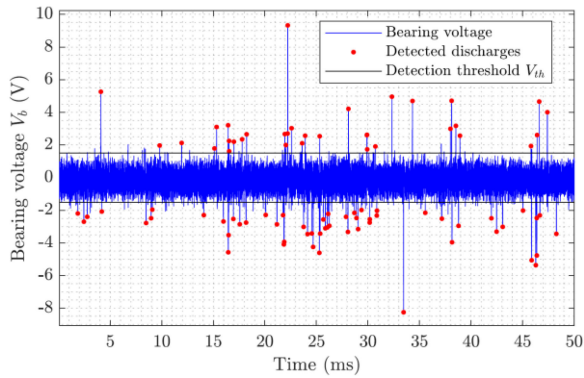


Fig. 5. Application of discharge detection algorithm on the measured bearing voltage V_b with the proposed setup: $V_{ex} = 10$ V; $f_{ex} = 10$ kHz; $F_{ech} = 12.5$ MS/s; $V_{th} = 1.5$ V.

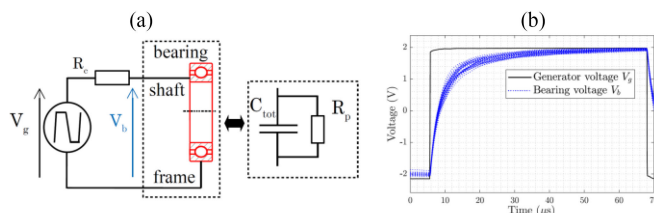


Fig. 6. Identification of the equivalent capacitance involved during an EDM process; (a) Circuit diagram; (b) Voltage waveforms.

D. Discharge Energy Estimation

To compute the energy of one discharge, we identified the equivalent capacitance C_{tot} of the test motor based on the method proposed in [41]. In our case, we can formulate $C_{tot} = C_{b,DE} + C_{rf}$ since the capacitance $C_{b,NDE}$ is neglected for a ceramic bearing. According to experimental results of [41], there is no significant speed influence on the bearing capacitance for bearing temperature between 20 °C and 40 °C. Thus, we assume that the capacitance C_{tot} is constant with speed variations (i.e. the variations of the lubricant film thickness with speed have a negligible effect on C_{tot} value). The motor had been running at its nominal speed for at least 60 min to insure bearing thermal steady-state around 22 °C. Then, the test bearing is submitted to a square wave voltage (2 V peak, 8 kHz) with a high output resistance R_c introduced to obtain a measurable time constant τ (Fig. 6). It should be noted that the applied voltage V_g is lower than the bearing breakdown voltage in order to prevent the occurrence of discharges. As the lubricant film is fully capacitive at nominal rotation speed, the equivalent capacitance C_{tot} is charged through the resistance R_c and can be identified through bearing voltage measurements by evaluating the time constant τ . To minimize the variations of the identified capacitances, an averaged value is computed on 30 pulses spaced of 500 ms, hence it is found $C_{tot} = 3.8$ nF at bearing temperature $T_b = 22^\circ\text{C}$. For $T_b = 33^\circ\text{C}$ (see Section VI.a), the capacitance increased to $C_{tot} = 6.4$ nF. The influence of the bearing load on the capacitance C_{tot} [42] is not considered since the bearing load is constant in all the following tests. The lubricant is generally modeled using a parallel resistance R_p [43] that can be neglected because the bearing voltage is about

equal to the applied voltage V_g (see Fig. 6(b)). Then, the energy W_{dis} dissipated in the bearing by capacitive discharges for a given time of operation t_{op} can be estimated using (4):

$$W_{dis}(t_{op}) = \frac{1}{2} C_{tot} \sum_{t_{op}} V_{bd}^2. \quad (4)$$

The measurement method, along with DA and energy estimations can be performed online on test-bench with minimum requirements.

E. Test Protocol

In order to analyze the influence of one single operating parameter on the discharge phenomenon (discharge activity and discharge energy), the bearing must be independent from the time of continuous operation or “history” of the motor which has a major impact on the DA [29]. This is reported to be linked to a change of microscopic properties in the lubricating zone, that reduce the overall dielectric strength of the lubricant [33]. Therefore, in this paper, all tests are time-spaced from at least 12 hours of inactivity of the motor. Moreover, it has been observed that in steady-state conditions (bearing thermal stabilization and constant rotational speed), the DA is far from being constant [29]. Thus, any change in the operating parameters is considered to have an influence on the DA and/or breakdown voltages only if a significant variation is observed. This will be analyzed in each following section: we apply the proposed measurement method (Sections III.C & III.D) during time of operation ranging from 90 to 360 min. The electrical stress is applied to the bearing as described in Section III.B for a constant bearing load. Note that the impact of the bearing load has previously been discussed in [28] on bearing current magnitude and in [15] on electrical bearing damage type (pitting or fluting of the raceways). In this work, the bearing steady-state conditions are defined by a constant bearing temperature at 1500 rpm. For discharge energy estimation, the capacitance C_{tot} is evaluated for different greases and bearing temperatures. For a wider range of operating conditions, a look-up table for the capacitance C_{tot} can be employed as proposed in [6] considering parameters such as load, grease type, speed and temperature.

IV. RESULTS 1: INFLUENCE OF BEARING VOLTAGE AMPLITUDE AND FREQUENCY

A. Bearing Voltage Amplitude

We study the influence of bearing voltage amplitude on both DA and discharge energy using variations of V_{ex} in the range 5 – 40 V. A square wave signal is applied on the bearing with the proposed setup as defined in Section III.B. The switching frequency is set at a typical industrial frequency of $f_{ex} = 10$ kHz. The motor is started up with $V_{ex} = 10$ V. In steady-state conditions around $t_{op} = 60$ min, V_{ex} is changed during motor operation while all other operating parameters are kept constant. Results of this test over time of operation are synthesized in Fig. 7 and Table I. To facilitate readability when the voltage is set to $V_{ex} = 10$ V, the discharge activity DA_m is also represented with its linear model (Fig. 7). The test

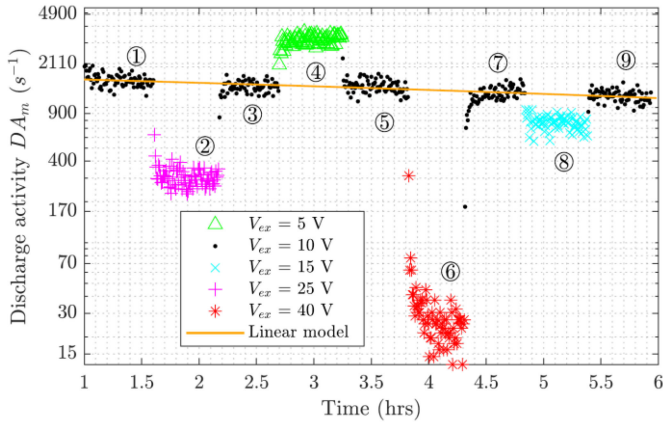


Fig. 7. Discharge activity measured for different excitation voltages applied at the test bearing with the proposed test protocol.

TABLE I
VARIATIONS OF ENERGY RELEASED IN THE BEARING BY CAPACITIVE DISCHARGES OVER THE 30 MIN INTERVALS OF FIG. 7

Time interval	1	2	3	4	5	6	7	8	9
V_{ex} (in V)	10	25	10	5	10	40	10	15	10
$W_{dis}(t_{op})^*$	1	0.19	0.74	0.22	0.92	0.02	0.76	0.56	0.7

* $W_{dis}(t_{op})$ is the absolute value of energy released over 30 min intervals with the first time interval being the reference value.

revealed that, when the excitation voltage is increased over 10 V (i.e. $V_{ex} = [15, 25, 40]$ V) both the DA and the released energy clearly decreased during these periods of time (Table I). This indicates that the lubricant is a non-linear impedance. The lubricant seems to have a more significant resistive behavior when the excitation voltage is increased. Therefore, a high voltage applied on the bearing do not imply the presence of high breakdown voltages. This is in line with the experimental results reported recently in [31], [44]. For $V_{ex} = 5$ V, the DA is increased compared to higher excitation voltages (Fig. 7) which suggests that the lubricant behaves mainly as a capacitor when the voltage is low. In this configuration, the discharge energy is however not increased (Table I). In our test, the chosen voltage variations (no linear increase/decrease of the voltage) reveal that the bearing lubricant is able to switch from capacitive to resistive mode and then to capacitive mode again.

For the lubricant of the test bearing, the given load, speed, and temperature, we found that the total energy released by capacitive discharges is at its maximum for a given excitation voltage around $V_{ex} \approx 10$ V, which seems the worst-case scenario in terms of bearing damage (high DA and high total energy dissipated in the bearing). In this case, the energy of the discharges is in the range of 25-110 nJ using (3). We noticed that the DA is maximum for an excitation voltage in the range $V_{ex} \approx [2, 5]$ V, and below 2 V, we observed that the lubricant is fully able to withstand the voltage. In the cases $V_{ex} = 25$ V and $V_{ex} = 40$ V, the maximum breakdown voltage is still $V_{bd} \approx 25$ V as observed in Section III.C, however, the DA continues to decrease for $V_{ex} = 40$ V. Above 40 V, the lubricant is mostly resistive with a few EDM events. This means

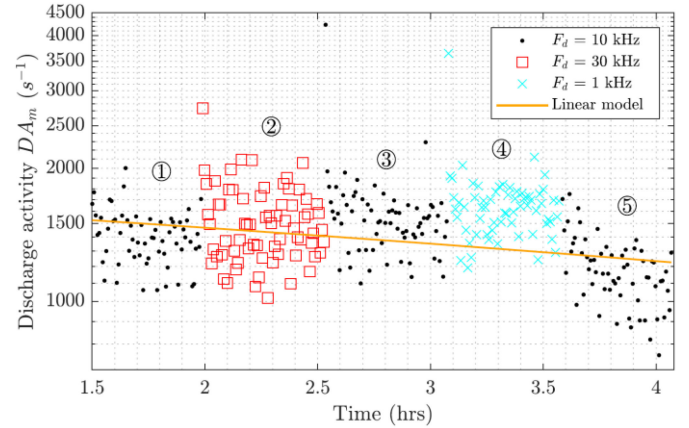


Fig. 8. Discharge activity measured for different excitation frequencies applied at the test bearing with the proposed test protocol.

that a theoretical maximum breakdown voltage obtained with the BVR (1) may not be reach since a breakdown depends on lubrication conditions. The most dangerous configuration is thus observed for $V_{ex} = 25$ V, because breakdown voltages up to 25 V are allowed, leading to high-energy discharges along with a higher DA than for $V_{ex} = 40$ V. In this case, we quantified that only 3.7 % of the events have a breakdown voltage higher than 10 V. Highest breakdown voltages are therefore scarce; however, they may lead to largest micro-craters on raceways [15] with discharge energy up to 1.2 μ J using (3).

B. Bearing Voltage Frequency

It has been found in [35] that the modification of the switching frequency does not influence magnitudes of EDM bearing currents. It is measured in [27] an increase of the discharge activity (i.e. a highest probability of EDM current) with the increase of the switching frequency of the drive in the range of 4 to 16 kHz. The work done in [29], [30] also showed a higher DA with an increase of the switching frequency in the range 1-4 kHz and 1-8 kHz respectively. Yet, a seemingly high DA is observed on a bearing directly submitted to a DC voltage [44], [45], as long as the bearing lubricant presents a capacitive behavior and the applied voltage is high enough to surpass the breakdown voltage of the lubricant. So, the influence of switching frequency on the DA , needed to be investigated from a fresh perspective.

An investigation is performed in order to observe the bearing response to different frequencies of the bearing voltage. To favor the presence of discharges, a square wave signal with $V_{ex} = 10$ V is applied on the bearing following the proposed setup defined in Section III.B. At the beginning of the test, the excitation frequency is set to $f_{ex} = 10$ kHz. Then, after the bearing reached its steady-state conditions, the excitation frequency is changed to a new value during 30 min (i.e. typical frequencies used in industry $f_{ex} = [1, 10, 30]$ kHz) while the motor is running with all other operating parameters kept constant. To facilitate readability when the frequency is set to $f_{ex} = 10$ kHz, the discharge activity DA_m is also represented with its linear model (Fig. 8). The results do not indicate a clear influence of the switching frequency on the DA . The probability distributions of

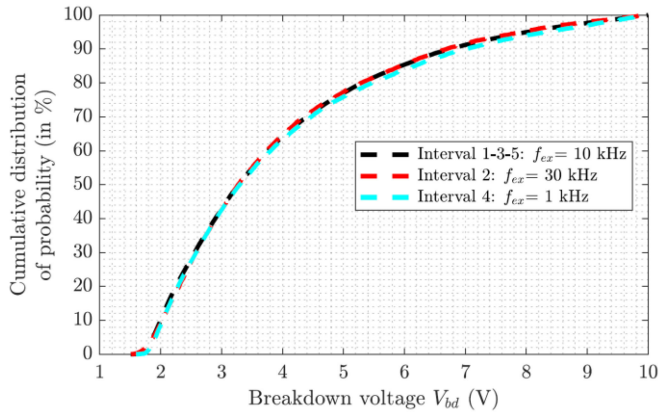


Fig. 9. Cumulative distribution of probability of the breakdown voltage for different excitation frequencies over the 30 min intervals of Fig. 8.

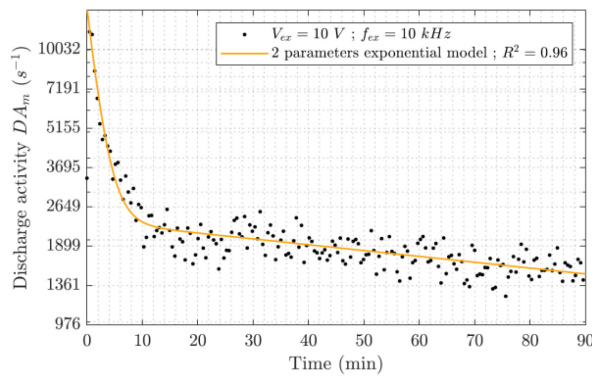


Fig. 10. Discharge activity measured at the startup of the motor with the proposed test protocol.

breakdown voltages are identical during the frequency variations (Fig. 9) and the mean breakdown voltage is rather constant, as well as the total energy released by capacitive discharges on each 30 min interval. Consequently, the bearing voltage frequency is found to neither influence the DA nor the discharge energy in the range 1 – 30 kHz. Thus, when considering bearing damage due to EDM bearing currents, the switching frequency of the inverter is not one of the influential parameters. To supplement this study, the impact on voltage time rise on breakdown voltage magnitude could be further investigated using various inverter modules.

V. RESULTS 2: STARTUP AND SUCCESSIVE STARTUPS TESTS

A. Startup Test

The excitation voltage is set to $V_{ex} = 10$ V to generate a sufficiently high DA (see Section IV.A) in order to analyze its variations. The excitation frequency is fixed to $f_{ex} = 10$ kHz which is a rather common switching frequency in the industry. The startup test showed that the DA is at its maximum at the start of the motor (Fig. 10) as reported in [29]. Then, the DA is exponentially decreasing even after the bearing reached its steady-state conditions around $t_{op} = 60$ min. We found that such decrease rate seems to be dependent on bearing type (see Section VI.B). Our statistical analysis also demonstrated that the

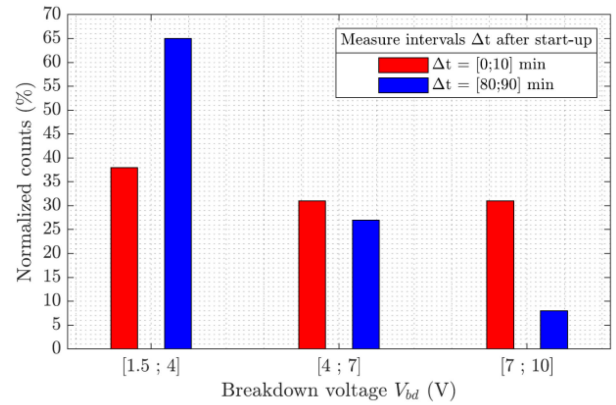


Fig. 11. Normalized counts of the discharges on two defined time intervals Δt after the startup.

TABLE II
CHARACTERISTIC VARIABLES OF THE STARTUP TEST

	$t_{op} = [0, 10] \text{ min}$	$t_{op} = [80, 90] \text{ min}$
$\langle DA_m \rangle_{t_{op}}^*$	$4.57 \times 10^3 \text{ s}^{-1}$	$1.58 \times 10^3 \text{ s}^{-1}$
$V_{bd,m}$	6.8 V	3.9 V
$W_{dis}(t_{op})$	267 mJ	33 mJ

* $\langle DA_m \rangle_{t_{op}}$ is the mean of DA_m over the duration t_{op} .

discharges are of higher energies for the first 10 min of operation than 80 min after the startup (Fig. 11). A decrease of the mean breakdown voltage $V_{bd,m}$ is observed during the test (Table II). The discharge energy W_{dis} is 8 times higher at startup than for steady-state conditions. We measured a variation of 0.1 nF for the capacitance C_{tot} during the startup test, so C_{tot} is assumed constant for discharge energy estimation (4). Hence, the startup of the machine is a critical state for the bearings: high DA with high breakdown voltages.

B. Successive Startups Test

It has been reported in [15] that the bearing electrical micro-pitting is more significant in variable speed mode than in constant speed mode. Similarly, an increase of the DA after startup phases is also reported in [29]. A new study is performed to quantify the DA and the discharge energy for duty cycle operation to supplement existing knowledge available in [15], [29]. A profile of 10 startups (2 min duration, 1 min deceleration) is performed (Fig. 12). The test can be associated to an IEC 60034-1 S5 operating condition (intermittent periodic duty but without electric braking). The initial DA maximal level is observed for each new startup of the motor. The energy released by capacitive discharges for each start is rather constant. During $t_{op} = 30$ min, we estimate a released energy of $W_{dis} \approx 760$ mJ which is largely superior to the released energy $W_{dis} \approx 102$ mJ during constant speed operation (Fig. 10) for the same duration ($t_{op} = [60, 90]$ min). Furthermore, we found that breakdown voltages remain at high values for each motor startup compared to steady-state conditions, which demonstrates that duty cycle operation is much more harmful for the bearing life than constant

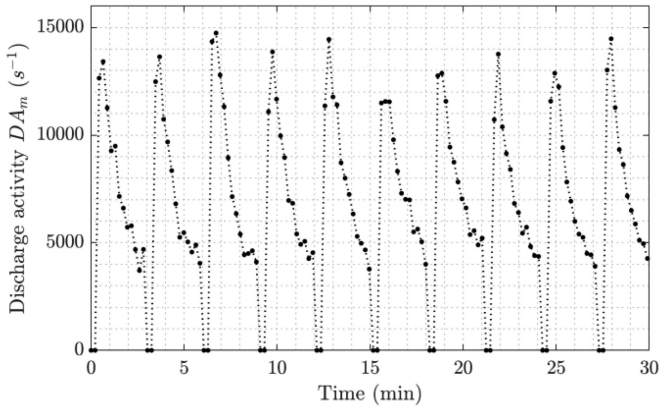


Fig. 12. Discharge activity measured for successive startups with the proposed test protocol.

speed operation. These tests provide a better insight in the discharge phenomenon from an electrical point of view. It has to be noted that, the behavior reported here was confirmed with other startup and duty cycle operation tests performed on the same bearing.

VI. RESULTS 3: INFLUENCE OF BEARING TEMPERATURE AND BEARING GREASE

A. Bearing Temperature

Results of [26], [31] exhibit non-linear variations of the DA in the speed-temperature plane. Maximum levels seem to be reached at certain speed-temperature points. Those points are not predictable since they also depend on lubricant and bearing voltage magnitude. DA variations with temperature are coupled with speed since a minimum speed is required for a given temperature for the establishment of an electrically insulating lubricant film [26]. Moreover, the reported tendency is a maximum of EDM-current magnitude at a certain motor speed which is reduced for an increase of bearing temperature and shifted to higher motor speed [28], [35].

Since no work provides simultaneously DA and discharge energy for some operating points, it is not possible to conclude that maximum DA levels lead to electrical bearing endangerment at some temperature levels. Thus, we propose to go further by evaluating both DA and discharge energy for different steady-state bearing temperatures. We have run two independent tests with two different temperatures. The motor is run at 1500 rpm during 90 min with a voltage ($V_{ex} = 10$ V and $f_{ex} = 10$ kHz) applied at the bearing as defined in Section III.B. At $t_{op} = 60$ min, the bearing temperature is stabilized at $T_b = 22^\circ\text{C}$ for the first test and $T_b = 33^\circ\text{C}$ for the second one. Note that these tests had been performed 3 times to insure the reproducibility of the result. For computation of discharge energy, the capacitance C_{tot} is measured at the two different temperatures prior to the tests (see Section III.D). The DA is slightly higher for $T_b = 22^\circ\text{C}$ than for $T_b = 33^\circ\text{C}$ (Fig. 13 and Table III). This behavior could be related to the increase of grease conductivity with temperature as observed recently in [31]. The bearing could present a more pronounced resistive mode with less possibilities for the voltage

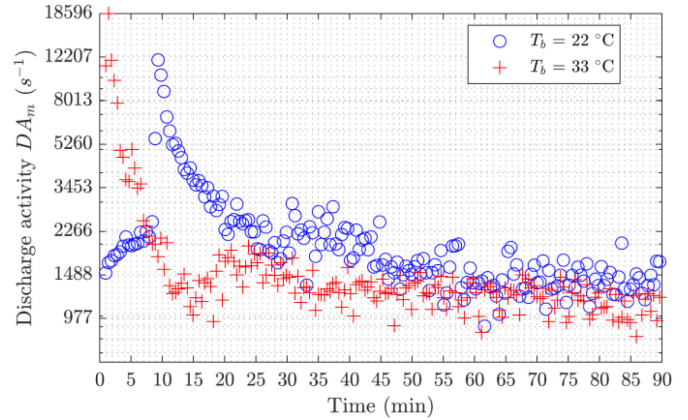


Fig. 13. Discharge activity measured for two different bearing temperatures with the proposed test protocol.

TABLE III
CHARACTERISTIC VARIABLES OF THE BEARING TEMPERATURE TEST

	$T_b = 22^\circ\text{C}$	$T_b = 33^\circ\text{C}$
$\langle DA_m \rangle_{t_{op}}^*$	$1.61 \times 10^3 \text{ s}^{-1}$	$1.15 \times 10^3 \text{ s}^{-1}$
$V_{bd,m}$	3.8 V	2.7 V
$W_{dis}(t_{op})$	89 mJ	31 mJ

* $\langle DA_m \rangle_{t_{op}}$ is the mean of DA_m over the duration $t_{op} = [60, 90]$ min.

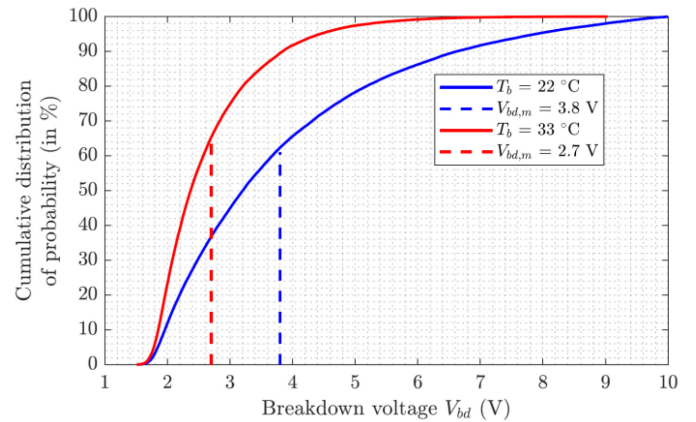


Fig. 14. Cumulative distribution of probability of the breakdown voltage over $t_{op} = [60, 90]$ min for two different bearing temperatures.

to build-up due to increase of grease conductivity. Our results are in line with the findings of [26], [31] where it is observed that the bearing goes progressively into a resistive mode as the temperature increases. Our experiment showed opposite results compared to [29] in which an elevated shaft temperature had led to an increase of the DA in steady-state conditions. This is probably caused by different operating speed and lubricant type. In addition, in our test, it is found that both the mean breakdown voltage $V_{bd,m}$ and the energy released by capacitive discharges W_{dis} are higher for $T_b = 22^\circ\text{C}$ (Fig. 14 and Table III).

Hence, for this test bearing at a motor speed sufficiently high to allow the establishment of an electrically insulating lubricant film, both DA and discharge energy are higher at lower bearing

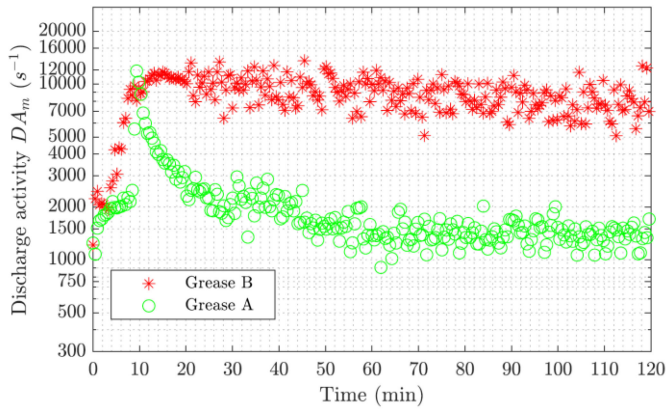


Fig. 15. Discharge activity measured for two different greases with the proposed test protocol at $T_b = 22^\circ\text{C}$.

temperature. However, it should be remembered that this result depends also on bearing voltage, speed and lubricant. So, for practical applications, an evaluation should be performed on typical operating modes to identify safest ones for longer bearing life.

B. Bearing Grease

We aim to compare two high resistivity lubricants typically used for life lubricated bearings to quantify the impact on DA and discharge energy. The grease A (from the test bearing presented previously) is used for standard applications with induction motor and is composed of mineral oil with a lithium soap thickener. The grease B (from another test bearing) is used for high temperature applications up to 160°C and is composed of an ester oil and a polyurea thickener. Prior to the tests, the capacitance C_{tot} is evaluated for both bearings in the same steady-state conditions with the protocol detailed in Section III.D. Hence, it is found $C_{tot} = 3.8\text{ nF}$ for grease A and $C_{tot} = 4.2\text{ nF}$ for grease B at $T_b = 22^\circ\text{C}$. A square wave signal ($V_{ex} = 10\text{ V}$ and $f_{ex} = 10\text{ kHz}$) is applied on the bearing with the proposed setup as defined in Section III.B. This procedure is repeated for the two different bearings during $t_{op} = 120\text{ min}$. In steady-state conditions for $t_{op} = [90, 120]\text{ min}$, it is observed that the DA of grease B is 5.6 times higher than the DA of grease A (Fig. 15). On this time interval, the mean breakdown voltage $V_{bd,m}$ is higher for grease B (Fig. 16 and Table IV). Furthermore, our results reveal that the decrease rate of both DA and breakdown voltage magnitudes are dependent of grease type. The estimation of the energy released by capacitive discharges showed that the bearing with grease B received almost 18 times more energy from discharges than the bearing with grease A for same time of operation $t_{op} = [90, 120]\text{ min}$ (Table IV). This section confirms the assumption of [46] with quantitative results and provides a more comprehensive approach to test bearing greases compared to [31].

Therefore, some bearings are prone to suffer from EDM bearing currents much more rapidly than other bearings under identical operating conditions. A direct solution of this issue would be the use of a grease with electrical properties close to grease A in order to mitigate the highest breakdown voltages to occur in the bearing.

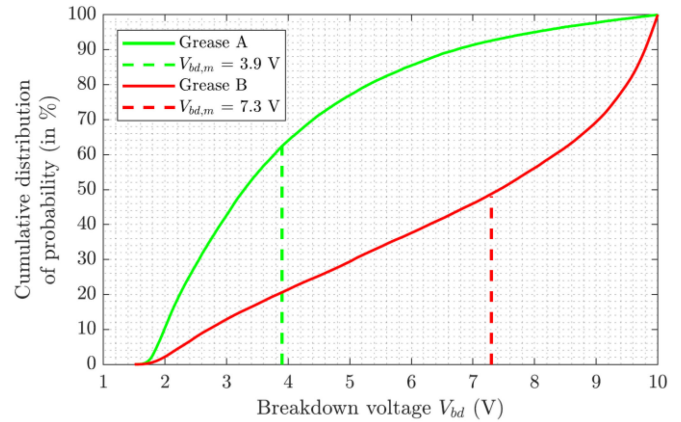


Fig. 16. Cumulative distribution of probability of the breakdown voltage over $t_{op} = [90, 120]\text{ min}$ for two different greases.

TABLE IV
CHARACTERISTIC VARIABLES OF THE GREASES TEST

	Grease A	Grease B
$\langle DA_m \rangle_{t_{op}}^*$	$1.61 \times 10^3\text{ s}^{-1}$	$7.97 \times 10^3\text{ s}^{-1}$
$V_{bd,m}$	3.9 V	7.3 V
$W_{dis}(t_{op})$	105 mJ	1840 mJ

* $\langle DA_m \rangle_{t_{op}}$ is the mean of DA_m over the duration $t_{op} = [90, 120]\text{ min}$.

VII. TEST BENCH VALIDATION

The measured discharges theoretically produce micropitting of the raceways resulting from fusion and vaporization of the materials. For standard bearing steel 100Cr6, considering a molten hemisphere volume from a crater of radius r (in m^3), it has been proposed in [15] the melting enthalpy (in J):

$$H_{\text{melting}} = 2.2 \cdot 10^{10} \cdot r^3 \quad (5)$$

Thus, breakdown voltages ranging from 1.5 to 25 V and leading to measured discharge energies from 4.3 nJ to 1.2 μJ , correspond theoretically to molten craters of diameters from to 1.2 μm to 7.6 μm . After the tests, a Scanning Electron Microscopy (SEM) analysis is performed on the bearing with grease A. The electrical micropitting is visible on both inner and outer rings with crater sizes up to 4 μm in diameter. The average diameter size is 1.7 μm . For the majority of test runs with $V_{ex} = 10\text{ V}$, the mean breakdown voltage was 3.9 V. This corresponds to a measured discharge energy of $W_{dis} = 29\text{ nJ}$ that correlates well with the theoretical energy $H_{\text{melting}} = 13.5\text{ nJ}$ required for the average crater size of 1.7 μm . This is without considering the possible vaporization of the metal and energy dissipation into the lubricant. Consequently, our setup allowed discharge bearing currents that are representative of low power motors fed by inverters.

VIII. CONCLUSION

We have performed bearing voltage measurements for several hours of bearing operation to gain more insight on the discharge phenomenon inside a bearing under different conditions. The

proposed measurement method allowed simultaneous estimation of discharge activity and discharge energy using an online discharge detection algorithm on the bearing voltage. The level of electrical stress applied on the bearing is representative of a low power motor (up to 20 kW) operated by an inverter. Even though it is well-known that the motor history has a strong impact on the discharge activity, diverse parameters strongly modify discharge activity and energy released by discharges in the bearing. We found that the magnitude of the bearing voltage plays a significant role on the lubricant's behavior. If the bearing voltage is too high, the discharge activity decreases. When the voltage on the bearing is set to 10 V, we observed a high *DA* and the total discharge energy is the highest compared to other voltages. For lower bearing voltage, the *DA* increases, and the discharges are of lower energy. For designing a motor-inverter system, ideally the common mode voltage and BVR should be as low as possible to reduce bearing endangerment due to EDM bearing currents. In such a configuration, the *DA* could still be high, but the energy of the discharges will be reduced, ideally with craters small enough to produce grey traces on raceways that are believed to not affect bearing life. The switching frequency of the bearing voltage, when observed independently, does not indicate a notable influence on neither the *DA* nor the breakdown voltages in the range 1-30 kHz.

The magnitude of breakdown voltages is found to depend on time of operation: high breakdown voltages at startup and lower breakdown voltages when the bearing reach steady-state conditions (constant temperature and speed). Duty cycle operation of the motor provokes a *DA* maximum level with high breakdown voltages after each startup compared to constant speed operation. An increase of the bearing temperature had led to lower breakdown voltages along with a lower *DA* in our experiments (with bearing grease A). Consequently, motors that run under heavy duty cycle operation, or at speed-temperature operating points that trigger high *DA* and/or high-energy discharges are more at risk to suffer from EDM bearing currents. Note that the BVR is known to be high in wound rotor motors [47], hence the bearings of such machines are more threatened due to high bearing voltage that leads to high-energy discharges. Applications such as variable speed pumps, HVAC fans, electric transportation systems have been found to suffer the most from EDM bearing currents from our experience.

We also witness that depending on grease type, a bearing can be submitted to both high discharge activity and high breakdown voltages over time of operation. The *DA* decrease over time of operation had also be found to depend on grease type.

Since EDM events and electrical properties of the grease are related to voltage magnitude, bearing temperature, operating mode, load and grease composition, a suitable bearing and/or mitigation technique can be selected depending on each motor application. For low-cost applications, a proper expertise on those influencing parameters are of importance in order to increase life of standard quality bearings. The knowledge of EDM bearing currents influencing parameters could also be considered for more accurate preventive maintenance. Further work on grease type selection under inverter operation would consist in a classification of electrical performances of the main greases used in industry.

REFERENCES

- [1] D. Busse, J. Erdman, R. J. Kerkman, D. Schlegel, and G. Skibinski, "System electrical parameters and their effects on bearing currents," *IEEE Trans. Ind. Appl.*, vol. 33, no. 2, Apr. 1997, Art. no. 2.
- [2] S. Bell *et al.*, "Experience with variable-frequency drives and motor bearing reliability," *IEEE Trans. Ind. Appl.*, vol. 37, no. 5, Oct. 2001, Art. no. 5.
- [3] R. Hoppler and R. Errath, "Motor bearings, not just a piece of metal," in *Proc. IEEE Cement Ind. Techn. Conf. Rec.*, Charleston, SC, USA, Apr. 2007, pp. 214–233.
- [4] A. Binder and A. Muetze, "Scaling effects of inverter-induced bearing currents in AC machines," *IEEE Trans. Ind. Appl.*, vol. 44, no. 3, Jun. 2008, Art. no. 3.
- [5] T. Dale, "Bearing damage in AC motors operating from PWM variable-frequency drives," Nidec Motor Corporation, Technical White Paper, EE Publishers, Jul. 2018.
- [6] M. Kriese, E. Wittek, S. Gattermann, H. Tischmacher, G. Poll, and B. Ponick, "Influence of bearing currents on the bearing lifetime for converter driven machines," in *Proc. 20th Int. Conf. Elect. Mach.*, Sep. 2012, pp. 1735–1739.
- [7] T. Hadden *et al.*, "A review of shaft voltages and bearing currents in EV and HEV motors," in *Proc. IECON-42nd Annu. Conf. IEEE Ind. Electron. Soc.*, Florence, Italy, Oct. 2016, pp. 1578–1583.
- [8] M. Schuster, J. Springer, and A. Binder, "Comparison of a 1.1 kW-induction machine and a 1.5 kW-PMSM regarding common-mode bearing currents," in *Proc. Int. Symp. Power Electron., Elect. Drives, Autom. Motion*, Jun. 2018, pp. 1–6.
- [9] T. Plazenet, T. Boileau, C. Caironi, and B. Nahid-Mobarakeh, "A comprehensive study on shaft voltages and bearing currents in rotating machines," *IEEE Trans. Ind. Appl.*, vol. 54, no. 4, Jul. 2018, Art. no. 4.
- [10] F. He, G. Xie, and J. Luo, "Electrical bearing failures in electric vehicles," *Friction*, vol. 8, no. 1, Feb. 2020, Art. no. 1.
- [11] S. Chen, T. A. Lipo, and D. Fitzgerald, "Source of induction motor bearing currents caused by PWM inverters," *IEEE Trans. Energy Convers.*, vol. 11, no. 1, Mar. 1996, Art. no. 1.
- [12] D. Busse, J. Erdman, R. J. Kerkman, D. Schlegel, and G. Skibinski, "Bearing currents and their relationship to PWM drives," *IEEE Trans. Power Electron.*, vol. 12, no. 2, Mar. 1997, Art. no. 2.
- [13] A. Muetze and A. Binder, "Practical rules for assessment of inverter-induced bearing currents in inverter-fed AC motors up to 500 kW," *IEEE Trans. Ind. Electron.*, vol. 54, no. 3, Jun. 2007, Art. no. 3.
- [14] O. Magdun, Y. Gemeinder, and A. Binder, "Prevention of harmful EDM currents in inverter-fed AC machines by use of electrostatic shields in the stator winding overhang," in *Proc. IECON-36th Annu. Conf. IEEE Ind. Electron. Soc.*, Glendale, AZ, USA, Nov. 2010, pp. 962–967.
- [15] H. Tischmacher and S. Gattermann, "Bearing currents in converter operation," in *Proc. 24th Int. Conf. Elect. Mach.*, Sep. 2010, pp. 1–8.
- [16] H. Prashad, "Chapter 4 Threshold voltage phenomenon and effect of operating parameters on the threshold voltage in rolling-element bearings," in *Tribology and Interface Engineering Series*, vol. 49, Amsterdam, Netherlands: Elsevier, 2006, pp. 71–87.
- [17] H. Prashad, "Chapter 11 Appearance of craters on track surface of rolling-element bearing by spark erosion," in *Tribology and Interface Engineering Series*, vol. 49, Amsterdam, Netherlands: Elsevier, 2006, pp. 225–242.
- [18] A. Muetze, A. Binder, H. Vogel, and J. Hering, "What can bearings bear?" *IEEE Ind. Appl. Mag.*, vol. 12, no. 6, pp. 57–64, Nov./Dec. 2006.
- [19] T. Zika, I. C. Gebeshuber, F. Buschbeck, G. Preisinger, and M. Gröschl, "Surface analysis on rolling bearings after exposure to defined electric stress," *Proc. Inst. Mech. Eng., Part J: J. Eng. Tribol.*, vol. 223, no. 5, May 2009, Art. no. 5.
- [20] A. Romanenko, A. Muetze, and J. Ahola, "Incipient bearing damage monitoring of 940-h variable speed drive system operation," *IEEE Trans. Energy Convers.*, vol. 32, no. 1, Mar. 2017, Art. no. 1.
- [21] H. Tischmacher, "Bearing Wear Condition Identification on Converter-fed Motors," in *Proc. Int. Symp. Power Electron., Elect. Drives, Autom. Motion*, Jun. 2018, pp. 19–25.
- [22] A. Becker and S. Abanteriba, "Electric discharge damage in aircraft propulsion bearings," *Proc. Inst. Mech. Eng., Part J: J. Eng. Tribol.*, vol. 228, no. 1, Jan. 2014, Art. no. 1.
- [23] D. F. Busse, J. M. Erdman, R. J. Kerkman, D. W. Schlegel, and G. L. Skibinski, "The effects of PWM voltage source inverters on the mechanical performance of rolling bearings," *IEEE Trans. Ind. Appl.*, vol. 33, no. 2, Apr. 1997, Art. no. 2.
- [24] K. Sunahara *et al.*, "Preliminary measurements of electrical micropitting in grease-lubricated point contacts," *Tribol. Trans.*, vol. 54, no. 5, Sep. 2011, Art. no. 5.

- [25] T. Didenko and W. D. Pridemore, "Electrical fluting failure of a tri-lobe roller bearing," *J. Fail. Anal. Preven.*, vol. 12, no. 5, Oct. 2012, Art. no. 5.
- [26] V. Niskanen, A. Muetze, and J. Ahola, "Study on bearing impedance properties at several hundred kilohertz for different electric machine operating parameters," *IEEE Trans. Ind. Appl.*, vol. 50, no. 5, Sep. 2014, Art. no. 5.
- [27] R. Smolenski, A. Kempinski, and J. Bojarski, "Statistical approach to discharge bearing currents," *COMPEL*, vol. 29, no. 3, May 2010, Art. no. 3.
- [28] O. Magdun, Y. Gemeinder, and A. Binder, "Investigation of influence of bearing load and bearing temperature on EDM bearing currents," in *Proc. IEEE Energy Convers. Congr. Expo.*, Sep. 2010, pp. 2733–2738.
- [29] A. Muetze, J. Tamminen, and J. Ahola, "Influence of motor operating parameters on discharge bearing current activity," *IEEE Trans. Ind. Appl.*, vol. 47, no. 4, Jul. 2011, Art. no. 4.
- [30] K. Khan and F. Gyllensten, "Experimental investigation of bearing currents in low voltage motors," in *Proc. 13th Int. Conf. Elect. Mach.*, Sep. 2018, pp. 218–224.
- [31] A. Gonda, R. Capan, D. Bechev, and B. Sauer, "The influence of lubricant conductivity on bearing currents in the case of rolling bearing greases," *Lubricants*, vol. 7, no. 12, Dec. 2019, Art. no. 12.
- [32] A. Muetze and A. Binder, "Calculation of motor capacitances for prediction of the voltage across the bearings in machines of inverter-based drive systems," *IEEE Trans. Ind. Appl.*, vol. 43, no. 3, May/Jun. 2007, Art. no. 3.
- [33] A. Romanenko, A. Muetze, and J. Ahola, "Effects of electrostatic discharges on bearing grease dielectric strength and composition," *IEEE Trans. Ind. Appl.*, vol. 52, no. 6, Nov. 2016, Art. no. 6.
- [34] V. Niskanen, "Radio-frequency-based measurement methods for bearing current analysis in induction motors," Ph.D. dissertation, Dept. Elect. Eng., Lappeenranta Univ. Technol., Lappeenranta, Finland, Dec. 2014.
- [35] A. Muetze, "Bearing currents in inverter-fed AC-motors," Ph.D. dissertation, Fachbereich Elektrotechnik und Informationstechnik, Technische Universität Darmstadt, Darmstadt, Germany, Jan. 2004.
- [36] J. A. Oliver, G. Guerrero, and J. Goldman, "Ceramic bearings for electric motors: Eliminating damage with new materials," *IEEE Ind. Appl. Mag.*, vol. 23, no. 6, Nov. 2017, Art. no. 6.
- [37] J. Ahola, A. Muetze, M. Niemela, and A. Romanenko, "Normalization-based approach to electric motor BVR related capacitances computation," *IEEE Trans. Ind. Appl.*, vol. 55, no. 3, May 2019, Art. no. 3.
- [38] J. Ahola, V. Särkimäki, A. Muetze, and J. Tamminen, "Radio-frequency-based detection of electrical discharge machining bearing currents," *IET Electric Power Appl.*, vol. 5, no. 4, 2011, Art. no. 4.
- [39] D. Hyypio, "Mitigation of bearing electro-erosion of inverter-fed motors through passive common-mode voltage suppression," *IEEE Trans. Ind. Appl.*, vol. 41, no. 2, Mar. 2005, Art. no. 2.
- [40] T. Plazenet, "Contribution à l'analyse de défauts de roulement induits par les défauts électriques de machines tournantes," Ph.D. dissertation, Université de Lorraine, France, Oct. 2019.
- [41] E. Wittek, M. Kriese, H. Tischnacher, S. Gattermann, B. Ponick, and G. Poll, "Capacitances and lubricant film thicknesses of motor bearings under different operating conditions," in *Proc. 14th Int. Conf. Elect. Mach.*, Rome, Italy, Sep. 2010, pp. 1–6.
- [42] E. Wittek, M. Kriese, H. Tischnacher, S. Gattermann, B. Ponick, and G. Poll, "Capacitance of bearings for electric motors at variable mechanical loads," in *Proc. 20th Int. Conf. Elect. Mach.*, Sep. 2012, pp. 1602–1607.
- [43] Y. Gemeinder, M. Schuster, B. Radnai, B. Sauer, and A. Binder, "Calculation and validation of a bearing impedance model for ball bearings and the influence on EDM-currents," in *Proc. Int. Conf. Elect. Mach.*, Sep. 2014, pp. 1804–1810.
- [44] A. Joshi and J. Blennow, "Investigation of the static breakdown voltage of the lubricating film in a mechanical ball bearing," *Proc. Nordic Insul. Symp.*, no. 23, Feb. 2018, Art. no. 23.
- [45] A. Jagenbrein, F. Buschbeck, M. Gröschl, and G. Preisinger, "Investigation of the physical mechanisms in rolling bearings during the passage of electric current," *Tribotest*, vol. 11, no. 4, Jun. 2005, Art. no. 4.
- [46] J. M. Erdman, R. J. Kerkman, D. W. Schlegel, and G. L. Skibinski, "Effect of PWM inverters on AC motor bearing currents and shaft voltages," *IEEE Trans. Ind. Appl.*, vol. 32, no. 2, Apr. 1996, Art. no. 2.
- [47] M. Whittle, J. Trevelyan, and P. J. Tavner, "Bearing currents in wind turbine generators," *J. Renew. Sustain. Energy*, vol. 5, no. 5, Sep. 2013, Art. no. 5.



Thibaud Plazenet received the Dipl.-Ing. degree in electrical engineering from the École Nationale Supérieure d'Électricité et de Mécanique, and the Ph.D. degree in electrical engineering from the Université de Lorraine, Nancy, France, in 2014 and 2019 respectively. He is currently a Postdoctoral Researcher at the Laboratoire d'Énergétique et de Mécanique Théorique et Appliquée, Nancy. His current research interests include maintenance of electric machines and fault diagnostics.



Thierry Boileau received the Ph.D. degree in electrical engineering from the Institut National Polytechnique de Lorraine, Nancy, France, in 2010.

In 2012, he joined the École Nationale Supérieure d'Électricité et de Mécanique, Université de Lorraine, Nancy, where he is currently an Associate Professor. From 2004 to 2017, he was at the Groupe de Recherche en Électrotechnique et Électronique de Nancy, Nancy. Since January 2018, he is with the Laboratoire d'Énergétique et de Mécanique Théorique et Appliquée, Nancy. His current research interests

include the diagnostics and control of electric machines supplied by power electronic converters, as well as electrothermal system control.



Cyrille Caironi (Member, IEEE) received the Dipl.-Ing. degree in electrical engineering and robotic, and the Ph.D. degree in physics from the Université de Lorraine, France, in 1998 and 2002, respectively.

From 1990 to 1999, he worked as CEO of a research and expertise firm before joining the ALSTOM group in 1999, where he was a Researcher and Development Manager until 2008. He was a Dean and Research Manager at CESI College of Engineers of Nancy, France, from 2008 to 2014. He is currently a Judicial Expert with French Tribunals, Managing Partner with

CAIRCY and CQO of PDSS GmbH (Power Diagnostic Service Switzerland). His main interests of research include monitoring and diagnostic of electrical machines.



Babak Nahid-Mobarakeh (Senior Member, IEEE) received the Ph.D. degree in electrical engineering from the Institut National Polytechnique de Lorraine (INPL), Nancy, France, in 2001. From 2001 to 2006, he was at the Centre de Robotique, Électrotechnique et Automatique, University of Picardie, Amiens, France. In September 2006, he joined the École Nationale Supérieure d'Électricité et de Mécanique, University of Lorraine, Nancy, where he worked as a Professor until December 2019. Since January 2020, he is a Professor at McMaster University, Hamilton, Canada. Dr. Nahid-Mobarakeh is the author or coauthor of more than 250 international peer reviewed journal and conference papers as well as several book chapters and patents. He has been the recipient of several IEEE awards. Dr. Nahid-Mobarakeh is the General Chair of the 2020 IEEE Transportation Electrification Conference and Expo (ITEC). Between 2012 and 2019, he served as Secretary, Vice Chair, Chair and Past Chair of the Industrial Automation and Control Committee (IACC) of the IEEE Industry Applications Society (IAS). He also was the IACC Committee Administrator and TCPRC.

His main research interests include nonlinear and robust control design of power converters and drives, fault detection and fault-tolerant control of electric systems, and design, control and stabilization of microgrids.